NASA TM-83262

NASA Technical Memorandum 83262

APPLICATION OF TWO-POINT DIFFERENCE SCHEMES TO THE CONSERVATIVE EULER EQUATIONS FOR ONE-DIMENSIONAL FLOWS

Stephen F. Wornom

MAY 1982

NASA
National Aeronautics and
Space Administration

Langley Research Center
Hampton, Virginia 23665

SUMMARY

An implicit finite-difference method is presented for obtaining steady-state solutions to the time-dependent, conservative Euler equations for flows containing shocks. The method uses the two-point differencing approach of Keller with dissipation added at supersonic points via the retarded density concept. Application of the method to the one-dimensional nozzle flow equations for various combinations of subsonic and supersonic boundary conditions shows the method to be very efficient. Residuals are typically reduced to machine zero in approximately 35 time steps for 50 mesh points. It is shown that the scheme offers certain advantages over the more widely-used three-point schemes, especially in regard to application of boundary conditions.

INTRODUCTION

Over the past decade much progress has been achieved in computing mixed subsonic-supersonic flows using the potential equation. Recent results by Jameson (ref. 1) using a multi-grid algorithm demonstrate the efficiency now achievable in obtaining accurate solutions to the potential equation. In order to avoid the irrotational assumption inherent in the use of the potential equation, attention is now being directed toward developing efficient methods for solving the conservative Euler equations. Since the conservative Euler equations

correctly model inviscid rotational flow and contain the Rankine-Hugoniot jump conditions, solutions with significant vorticity and/or strong shocks can be computed more accurately than those obtained using the potential equation.

Stability and convergence of numerical solutions to the Euler equations appear to be sensitive to the boundary conditions imposed. This is pointed out, for example, by Moretti (ref. 2) in regard to the calculations of Cline (ref. 3) for nozzle flows. This sensitivity is also seen in the numerical results of Yee, Beam, and Warming (ref. 4) who examined the effect of different boundary approximations on stability for implicit schemes which have as their basis a three-point central difference approximation for the Euler flux terms. Their study was motivated by the extra numerical boundary conditions, in addition to the physical ones, that are required by the three-point formulation in order to close the system of difference equations. This can be illustrated using the one-dimensional Euler equations which consist of the conservation of mass, momentum, and energy. Written in nonconservation form, the characteristic slopes in the (x,t) plane are u, $u \pm c$. If one considers the case where the inflow and outflow conditions are subsonic, there will be two incoming characteristics at the inflow boundary and one at the outflow boundary. This implies that only three physical boundary conditions are necessary to solve the three partial-differential equations--two at the entrance and one at the exit. However, the use of a three-point difference representation for the flux terms requires six numerical boundary conditions because the difference equations can be applied only at the interior mesh points. Thus, either extra numerical boundary conditions or some other treatments at the boundaries are required. This necessity for extra conditions can be satisfied in

several ways: (1) Specifying all conditions at the boundaries, (2) additional differencing of selected conservation laws at the boundaries, (3) using spatial extrapolations or time-spatial extrapolations at the boundaries, or (4) a combination of the above. These auxiliary conditions may be applied in an explicit or implicit manner. The paper by Yee, Beam, and Warming (ref. 4) examined the stability effects using all these possibilities. Every class of flow examined in reference 4 required extra numerical boundary conditions in addition to the physical ones.

In order to avoid this need for extra numerical boundary conditions, we examine in this report the idea proposed by Keller (ref. 5) of writing any system of differential equations as a first-order differential system and then representing all derivatives by a two-point approximation; that is, $(F_x)_{i-\frac{1}{2}} = (F_i - F_{i-1})/\Delta x$. This concept was applied by Keller and Cebeci (ref. 6) to solve the boundary-layer equations, which contain terms like u_{yy}. In order to write terms of this form as a first derivative, it was necessary to introduce a new variable, say $s \equiv u_y$, so that u_{yy} becomes s_y. The resulting two-point finite-difference equations were accurate to order Δy^2. Later, Wornom (ref. 7) provided a simple and efficient extension of Keller's idea which is of order Δy^4 accuracy for the boundary-layer equations. This extension still avoids the need for extra numerical boundary conditions required by three-point methods.

The two-point differencing idea appears to be a very attractive choice for numerically solving natural first-order systems, such as the Euler equations, for several reasons. First, since the system contains only first derivatives, there is no need to introduce new dependent variables as was necessary for the boundary-layer equations

which contained second derivatives. Second, the two-point difference equations, when applied to solve the mass, momentum, and energy equations without added dissipation terms, require only three boundary conditions to close the system; thus, for cases where three physical boundary conditions exist, the difficulties introduced at boundaries with a three-point method do not occur. The case of subsonic inflow and subsonic outflow is an example of a flow where three physical boundary conditions exist. However, there are also flow situations where the number of boundary conditions required to close the two-point system is larger than the number of physical boundary conditions available. These situations will also be addressed in this report.

SYMBOLS

A	cross-sectional nozzle area
A_i, B_i, C_i	coefficients in block tri-diagonal system defined in equations (19b)
$a_{11}, a_{12}, a_{21}, a_{22}$	coefficients appearing in equations (15) and (17)
$b_{11}, b_{12}, b_{21}, b_{22}$	coefficients appearing in equations (15) and (17)
c_{11}	coefficient appearing in equation (15)
c	nondimensional speed of sound, $c^2 = \gamma P/\rho$
$d_i^{(1)}, d_i^{(2)}, e_i^{(1)}, e_i^{(2)}$	coefficients in solution algorithm; defined in equations (20)
E	nondimensional total energy times cross-sectional area

$f_i^{(1)}, f_i^{(2)}$	steady-state residuals; see equations (15) and (17)
g_I, h_I	coefficients in boundary-condition equation (26c)
I	total number of mesh points
M	Mach number
P	nondimensional pressure times cross-sectional area
R	residual norm; see equation (29)
S	constant appearing in equation (24); related to entropy
t	time coordinate
T	nondimensional temperature (or enthalpy)
u	nondimensional longitudinal velocity component
x	axial space coordinate
ρ	nondimensional density times cross-sectional area except in figures where it is the physical density
$\bar{\rho}$	retarded density times cross-sectional area; see equations (12)
γ	ratio of specific heats
$\Delta\rho, \Delta u, \Delta\bar{\rho}$	change with respect to time coordinate
Δx	mesh spacing
Δt	time step
μ	switch function defined in equation (12c)
Z	matrix defined by equation (20c)

Subscripts

c	reference quantity in switch-function definition
i	index counter in x-coordinate mesh
r	reference quantity, nozzle entrance
total	denotes upstream reservoir condition
t	partial differentiation with respect to t
x	partial differentiation with respect to x

Superscripts

n	denotes time level
T	denotes matrix transpose
$(\bar{\ })$	denotes retarded quantity
-1	denotes matrix inverse

GOVERNING EQUATIONS

The governing equations are the quasi-one-dimensional, time-dependent Euler equations which define flow through a nozzle. These are written in conservation form as

$$\rho_t + (\rho u)_x = 0 \qquad \text{(mass)} \qquad (1)$$

$$(\rho u)_t + (P + \rho u^2)_x - \frac{P}{A} A_x = 0 \qquad \text{(momentum)} \qquad (2)$$

$$E_t + \left[(P + E)u\right]_x = 0 \qquad \text{(energy)} \qquad (3)$$

with

$$P = (\gamma - 1)\left[E - \frac{1}{2}\rho u^2\right] \qquad \text{(gas law)} \qquad (4)$$

where ρ, P, and E are the density, pressure, and total energy times the nozzle cross-sectional area $A(x)$. (See fig. 1.) ρ and u have been nondimensionalized by ρ_r and u_r and P and E by $\rho_r u_r^2$ where r denotes the entrance values. γ is the ratio of specific heats.

In this report only the steady-state solution is of interest, when it exists. Thus, the pressure is eliminated by integrating the steady-state energy equation taking the total enthalpy to be constant. The system of equations to be solved thus reduces to

$$\rho_t + (\rho u)_x = 0 \qquad \text{(mass)} \qquad (5)$$

$$(\rho u)_t + (P + \rho u^2)_x = \frac{P}{A} A_x \qquad \text{(momentum)} \qquad (6)$$

and

$$p = \frac{(\gamma - 1)}{\gamma} \rho \left(T_{total} - \frac{1}{2} u^2 \right) \tag{7}$$

where T_{total} is the nondimensional reservoir stagnation temperature (or enthalpy). If equations (5) and (6) are written in quasilinear form, these equations will have two characteristics with slopes given by

$$\frac{dx}{dt} = \frac{(\gamma + 1)u \pm \sqrt{(\gamma + 1)^2 u^2 - 4\gamma(u^2 - c^2)}}{2\gamma} \tag{8}$$

The directionality of the two characteristics is determined by the sign of equation (8) which is the same as the sign of $u \pm c$ where c is the local isentropic sound speed. The directionality of the characteristics at the boundary points will be used in a later section to determine how many boundary conditions may be applied at each boundary.

FINITE-DIFFERENCE EQUATIONS

The partial-differential equations (5) and (6) are replaced with the following two-point central-difference approximation:

$$\frac{1}{2} \left[\bar{\rho}_t \Big|_i + \bar{\rho}_t \Big|_{i-1} \right] + \left[(\bar{\rho}u)_i - (\bar{\rho}u)_{i-1} \right] \Big/ \Delta x = 0 \tag{9}$$

$$\frac{1}{2} \left[(\rho u)_t \Big|_i + (\rho u)_t \Big|_{i-1} \right] + \left[(P + \rho u^2)_i - (P + \rho u^2)_{i-1} \right] \Big/ \Delta x$$

$$- \frac{1}{2} \left[\left(\frac{P}{A} \right)_i + \left(\frac{P}{A} \right)_{i-1} \right] (A_i - A_{i-1}) \Big/ \Delta x = 0 \tag{10}$$

with

$$p_i = \frac{(\gamma - 1)}{\gamma} \rho_i \left(T_{total} - \frac{1}{2} u_i^2 \right) \tag{11}$$

where Δx = constant = $x_{max}/(I-1)$, $x_i = (i-1)\Delta x$, $i = 1,2,\ldots I$. $\overline{\rho}$ is a retarded density used to introduce dissipation at supersonic points. This idea was developed independently by Hafez, South, and Murman (ref. 8) and Holst and Ballhaus (ref. 9) for obtaining solutions to the potential equation. The retarded density is given by

$$\overline{\rho} = \rho - \mu \rho_x \Delta x \tag{12a}$$

or

$$\overline{\rho}_i = \rho_i - \mu_i (\rho_i - \rho_{i-1}) \tag{12b}$$

where

$$\mu_i = \max \left[0, 1 - (M_c / M_{i-\frac{1}{2}})^2 \right] \tag{12c}$$

M_c is a reference Mach number and $M_{i-\frac{1}{2}}$ is the mid-cell value (taken as the average of M_i and M_{i-1}).

The retarded density method was chosen for two reasons. First, the solution algorithm can be written so that the extra mesh point introduced by the dissipation at supersonic points does not alter the solution algorithm; and, second, using the retarded density, dissipation is only added at points where $M_{i-\frac{1}{2}} > M_c$ (supersonic or near-supersonic points).

The coefficient μ_i given by equation (12c) is not unique for the Euler equations. Other forms for μ_i were tried before selecting equation (12c). Equation (9) is linearized by Newton's method which

is achieved by letting

$$\bar{\rho}^n = \bar{\rho}^{n-1} + \Delta\bar{\rho} \tag{13a}$$

$$u^n = u^{n-1} + \Delta u \tag{13b}$$

and substituting these into equation (9). Neglecting terms of second order (e.g., $\Delta\bar{\rho} \cdot \Delta u$) this linearized equation can be written solely in terms of $\Delta\rho$ and Δu by eliminating the $\Delta\bar{\rho}$ terms using

$$\Delta\bar{\rho}_i = \Delta\rho_i - \mu_i^{n-1} (\Delta\rho_i - \Delta\rho_{i-1}) \tag{14}$$

For simplicity the value of the switch function μ_i is frozen at the previous time step. It is multiplied by a density difference which is $0(\Delta x)$ except across discontinuities; ignoring the dependence of μ on ρ and u in the linearization does not hinder convergence of the present algorithm. The desired approximation of the continuity equation is given by

$$b_{11}\Delta\rho_i + b_{12}\Delta u_i + a_{11}\Delta\rho_{i-1} + a_{12}\Delta u_{i-1} + c_{11}\Delta\rho_{i-2} = f_i^{(1)} \tag{15}$$

where

$$b_{11} \equiv \left[u_i^{n-1}/\Delta x + \frac{1}{2\Delta t}\right]\left(1 - \mu_i^{n-1}\right) \tag{16a}$$

$$b_{12} \equiv \bar{\rho}_i^{n-1}/\Delta x \tag{16b}$$

$$a_{11} \equiv -\left[u_{i-1}^{n-1}/\Delta x - \frac{1}{2\Delta t}\right]\left(1 - \mu_{i-1}^{n-1}\right) + \left[u_i^{n-1}/\Delta x + \frac{1}{2\Delta t}\right]\mu_i^{n-1} \tag{16c}$$

$$a_{12} \equiv -\bar{\rho}_{i-1}^{n-1}/\Delta x \tag{16d}$$

$$c_{11} \equiv - \left[u_{i-1}^{n-1} \Big/ \Delta x - \frac{1}{2\Delta t} \right] \mu_{i-1}^{n-1} \tag{16e}$$

$$f_i^{(1)} \equiv - \left[(\bar{\rho u})_i^{n-1} - (\bar{\rho u})_{i-1}^{n-1} \right] \Big/ \Delta x \tag{16f}$$

To write the momentum equation in a similar form, we approximate the time term $(\rho u)_t$ as $\rho^{n-1} u_t + u^{n-1} \rho_t$. Inserting $\rho^n = \rho^{n-1} + \Delta\rho$ and $u^n = u^{n-1} + \Delta u$ and equation (11) into the momentum equation yields a linearized momentum equation with the same form as equation (15), that is

$$b_{21}\Delta\rho_i + b_{22}\Delta u_i + a_{21}\Delta\rho_{i-1} + a_{22}\Delta u_{i-1} = f_i^{(2)} \tag{17}$$

The coefficients in equation (17) are left as an exercise to the reader.

Note that equations (15) and (17) are compact in that only two points are used in subsonic regions and three points in supersonic regions (continuity equation only). In the next section, an algorithm is presented for solving the system of implicit difference equations, equations (15) and (17), assembled over all cells.

SOLUTION ALGORITHM

Equations (15) and (17) can be written as a block tridiagonal system which can be inverted using a block tridiagonal solver. Normally, a tridiagonal system involves three mesh points where i+1, i, and i-1 would be the three diagonal terms. However, for the two-point system, the diagonal terms refer to different groupings of the dependent variables and not to separate mesh points. Block tridiagonal

solvers are applied in two recursive steps, one a forward sweep and the other a back substitution.

The back-substitution step, used here is taken as:

$$\Delta\rho_i = d_i^{(1)} + e_i^{(1)}\Delta u_i \qquad (18a)$$

$$i = I,\ I-1,\ \ldots\ 2$$

$$\Delta u_{i-1} = d_i^{(2)} + e_i^{(2)}\Delta u_i \qquad (18b)$$

This step is applied in a recursive manner for decreasing values of i (right-to-left sweep) and used the coefficients $d_i^{(1)}$, $e_i^{(1)}$, $d_i^{(2)}$, and $e_i^{(2)}$ which are computed from the forward step (left-to-right sweep).

The block tridiagonal system inverted with this solver is obtained by writing equations (15) and (17) as

$$A_i(\Delta\rho_{i-2}, \Delta\rho_{i-1})^T + B_i(\Delta\rho_i, \Delta u_{i-1})^T + C_i\Delta u_i = \left[f_i^{(1)}, f_i^{(2)}\right]^T \qquad (19a)$$

where

$$A_i = \begin{bmatrix} c_{11} & a_{11} \\ 0 & a_{21} \end{bmatrix};\ B_i = \begin{bmatrix} b_{11} & a_{12} \\ b_{21} & a_{22} \end{bmatrix};\ C_i = \begin{bmatrix} b_{12} \\ b_{22} \end{bmatrix} \qquad (19b)$$

and $(\Delta\rho_{i-2},\ \Delta\rho_{i-1})^T$, $(\Delta\rho_i, \Delta u_{i-1})^T$, and Δu_i are the three diagonal terms. Other groupings of dependent variables are possible and, therefore, the algorithm given by equations (18) is not unique.

The coefficients $d_i^{(1)}$, $d_i^{(2)}$, $e_i^{(1)}$, and $e_i^{(2)}$ are obtained by using equations (18) to eliminate the lower diagonal terms in equations (19), the coefficients are

$$\left[e_i^{(1)},\ e_i^{(2)}\right]^T = -\ Z_i^{-1}C_i \qquad i = 2,\ 3,\ \ldots,\ I-1, I \qquad (20a)$$

$$\left[d_i^{(1)},\ d_i^{(2)}\right]^T = Z_i^{-1}F_i \tag{20b}$$

where

$$F_i = \left[f_i^{(1)} - c_{11}\left(d_{i-2}^{(1)} + e_{i-2}^{(1)}d_{i-1}^{(2)}\right) - a_{11}d_{i-1}^{(1)},\ f_i^{(2)} - a_{21}d_{i-1}^{(1)}\right]^T$$

and

$$Z_i = \begin{bmatrix} b_{11} & a_{12} + c_{11}e_{i-2}^{(1)}e_{i-1}^{(2)} + a_{11}e_{i-1}^{(1)} \\ b_{21} & a_{22} + a_{21}e_{i-1}^{(1)} \end{bmatrix} \tag{20c}$$

These coefficients are computed in a recursive manner with increasing i (left-to-right sweep), the forward step. In order to start this sweep, the coefficients $d_0^{(1)}$, $e_0^{(1)}$, $d_1^{(1)}$, and $e_1^{(1)}$ must be known. They are obtained from the boundary conditions as discussed in the next section.

After the coefficients are computed in the forward sweep, the back-substitution sweep is initiated using the outflow boundary condition to determine Δu_I. This is done by setting the terms resulting from the solution algorithm for $\Delta\rho_I$ equal to those derived from the exit boundary condition. (See next section.) That is,

$$\Delta\rho_I = d_I^{(1)} + e_I^{(1)}\Delta u_I = g_I + h_I\Delta u_I \tag{21}$$

(algorithm) (boundary condition)

Solving for Δu_I we obtain

$$\Delta u_I = \left[d_I^{(1)} - g_I\right] \Big/ \left[h_I - e_I^{(1)}\right] \tag{22}$$

BOUNDARY CONDITIONS

Difference equations (15) and (17) are to be applied on the grid shown in figure 2 where $i = 1$ is the inflow boundary and $i = I$ is the outflow boundary. The number of boundary conditions required to close the system of difference equations can be determined from the following relation:

Total number of difference equations + number of boundary conditions = (number of dependent variables) · (number of mesh points) (23a)

The two difference equations (mass, momentum) can be applied in all cells; therefore, the total number of difference equations is $2(I - 1)$. Thus, equation (23a) becomes

$$2(I - 1) + \text{number of boundary conditions} = 2 \cdot I \tag{23b}$$

and it appears that two boundary conditions are required to close the system of difference equations. However, if supersonic inflow exists, three boundary conditions will be required because to retard the density at $i = 1$, the density at the "dummy" point $i = 0$ is required $\left[\bar{\rho}_1 = \rho_1 - \mu_1(\rho_1 - \rho_0)\right]$. Also M_0 is needed to compute μ_1 using equation (12c).

Next we examine whether the number of physical boundary conditions available are sufficient to satisfy the numerical boundary conditions required by the difference equations.

Subsonic Inflow

The characteristics for this case are shown in figure 3, where $M = u/c$ is the Mach number and dt is a differential time. For

this case, there exists both an incoming and an outgoing characteristic. The single incoming characteristic can be replaced by an arbitrary boundary condition. Here, the boundary condition is taken to be

$$(P_1/A_1) \Big/ (\rho_1/A_1)^{\gamma} = S_{total} \tag{24}$$

where S_{total} is a constant based on reservoir conditions. Recall that P and ρ are the physical pressure and density times the cross-sectional area.

Subsonic Outflow

The characteristics for this case are similar to the subsonic inflow. The incoming characteristic from downstream is replaced by

$$P_I = P_{exit} \tag{25}$$

where $i = I$ is the location of the outflow boundary.

Supersonic Inflow

The characteristics for this case are shown in figure 4. The two incoming characteristics can be replaced by two arbitrary boundary conditions. The entropy condition given in equation (24) is used as one of these boundary conditions and ρ_0 is taken as the other.

Supersonic Outflow

The characteristics for this case are similar to the inflow case but are outgoing characteristics; and, therefore, no boundary conditions should be specified at this boundary.

Table I summarizes the number of physical boundary conditions available for four classes of flow as well as the number of boundary conditions required by the present two-point method. It can be seen from Table I that the two-point scheme is ideally suited for class 1 and 3 flows since the number of physical boundary conditions available equals the number of boundary conditions required to close the two-point system and these can be applied at the appropriate boundaries. For flows where the outflow is supersonic (classes 2 and 4), the two-point method requires one more boundary condition to close the system than there are physical boundary conditions available. The additional boundary condition needed for closure when the outflow is supersonic is taken to be the exit pressure. The consequence of this over-specification of the downstream boundary will be discussed in the section devoted to numerical results.

In order to apply the boundary conditions to the difference equations, they are written in the following forms:

$$\Delta\rho_0 = d_0^{(1)} + e_0^{(1)}\Delta u_0 \qquad \text{(supersonic inflow only)} \tag{26a}$$

$$\Delta\rho_1 = d_1^{(1)} + e_1^{(1)}\Delta u_1 \tag{26b}$$

$$\Delta\rho_I = g_I + h_I\Delta u_I \tag{26c}$$

where d and e are superscripted so as to be consistent with the solution algorithm presented in the previous section. Equation (26a) is applied as a Dirichlet boundary condition, ρ_0 = constant; thus

$$d_0^{(1)} = e_0^{(1)} \equiv 0$$

In order to write boundary conditions (24) and (25) in the form of equations (26b) and (26c), we linearize the boundary conditions via Newton's method. This is accomplished by linearizing the boundary conditions (24) and (25) after eliminating the pressure with equation (11) and retaining only terms of order $\Delta\rho$ and Δu. Then the coefficients in equations (26b) and (26c) are:

$$d_1^{(1)} = -\rho_1 \left[P_1 - A_1(\rho_1/A_1)^{\gamma} S_{total} \right] \Big/ D_1 \tag{28a}$$

$$e_1^{(1)} = \frac{\gamma - 1}{\gamma} \rho_1^2 u_1 \Big/ D_1 \tag{28b}$$

$$D_1 = P_1 - \gamma A_1(\rho_1/A_1)^{\gamma} S_{total} \tag{28c}$$

$$g_I = \rho_I \left(\frac{P_{exit} - P_I}{P_I} \right) \tag{28d}$$

$$h_I = \rho_I u_I \Big/ \left(T_{total} - \frac{1}{2} u_I^2 \right) \tag{28e}$$

Recall that Δu_I is given by equation (22). All quantities in equations (28) are evaluated at the previous time level. The superscript n-1 has been omitted for simplicity.

NUMERICAL RESULTS

The present method was applied to compute flow through the nozzles shown in figure 5. Table II summarizes the five flow conditions investigated. These are the same cases investigated by Yee, Beam,

and Warming (ref. 4) using a three-point method. The initial conditions were obtained by linearly interpolating the velocity between the exact entrance and exit values and determining the density such that $\rho_i = (\rho u)_{exact}/u_i$. Linearly interpolating both density and velocity was also tried. The rate of convergence was unaffected by the choice of initial conditions.

Subsonic Flow--No Shock (Case I)

The convergence rate and Mach number profiles for the symmetric case are shown in figure 6. The residual shown in figure 6(a) and later figures is the maximum residual defined by

$$R \equiv \max \left[|f_i^{(1)}|_{max} , |f_i^{(2)}|_{max} \right] \tag{29}$$

Cases I and II are ideal for the two-point scheme since the number of physical boundary conditions equals the number of boundary conditions required to close the system of difference equations and they are applied at the appropriate boundaries (cf. Table I, classes 1 and 3).

This same case--when computed with a three-point method (ref. 4)--was the most sensitive (of all five cases) to the type of extra boundary conditions required by the three-point method. This is due to the throat being the only sonic point. Two types of extra numerical boundary conditions imposed on the three-point scheme produced converged solutions with shocks when a CFL (Courant, Fredricks, and Lewy) number > 1 was used. A $CFL_{max} = 1{,}000$ calculation was reported with the three-point method with a profile given at 500 time steps.

The results shown in figure 6 were obtained with a $CFL_{max} = 10^8$. Accurate profiles were reached in 10 time steps. The reference Mach

number, M_c, used to compute the retarded density with equations (12) was 1.0. When a value $M_c = 0.9$ was used, the convergence rate was unaffected but the local solutions at which $M_i \geq 0.9$ were smoothed due to the added dissipation.

Subsonic Flow--With Shock (Case II)

The convergence rate, Mach number, and density profiles for this case are given in figure 7. The density ρ_{total} is the value of total density upstream of the shock. The density, ρ, shown in the figures is the physical value. This represents an inconsistency since previously it was defined as the physical value times the cross-sectional area. The value of M_c for this case and all other cases was 0.9. A value of $M_c < 1$ was necessary for transonic flows in order to introduce sufficient artificial viscosity at the sonic point to prevent an expansion shock from occurring there. The Mach number and density profiles are shown after 10 time steps. According to reference 4, the maximum CFL number for this case using a three-point method was 20; whereas, the present calculations were computed with a maximum CFL of 10^8. However, no noticeable change in the convergence rate was observed for $CFL_{max} > 1{,}000$ for all test calculations. On this grid (65 points), the residuals were reduced to machine zero in approximately 45 time steps with the largest residual always occurring at the shock. As in the other cases, plotting accuracy was achieved in 10 time steps.

Subsonic Inflow--Supersonic Outflow (Case III)

The convergence rate and density profile for this case are shown in figure 8. This case is of particular interest for the present method since a downstream boundary condition (pressure) is prescribed where physically none should be prescribed. The results presented in figure 8

demonstrate the method to be accurate and have fast convergence for this case.

The results shown in figure 9 test the effect of applying a downstream boundary condition by lowering the downstream pressure below the supersonic expansion value. Physically, any pressure below this value should have no effect on the solution in the nozzle. As seen from figure 9, the effect of this boundary condition is restricted to a small "boundary-layer" region near the outflow boundary. This boundary-layer region is caused by the artificial dissipation introduced by the retarded density.

Supersonic Inflow--Subsonic Outflow (Case V)

The convergence rate, Mach number, and density profiles for this case are shown in figure 10. As noted previously, in order to use the retarded density for flows where the inflow is supersonic, the density and Mach number at the previous station must be specified. The values of ρ_0 and M_0 used were obtained from the exact solution. Again, according to reference 4, the maximum experimental CFL number for the three-point method was 10. The experimental maximum CFL number for the present calculations was approximately 250. As with the other cases, plotting accuracy was achieved in 10 time steps and the residuals reduced to machine zero in approximately 35 time steps.

Since this was the only test case for which the upper limit for the CFL number was less than 10^6 (see Table III), more numerical experiments were carried out. It was found that virtually unlimited Δt could be used by starting with a moderate value of Δt (corresponding to, say, CFL = 250) and increasing rapidly. A few such

experiments showed convergence to machine zero could be obtained in less than 30 steps.

Overall Comparison With Three-Point Method

Table III shows a comparison between the experimental maximum stable CFL numbers for all five test cases for both the three-point method (ref. 4) and the present method. For this comparison, 50 mesh points were used with the following sampling of CFL numbers: 0.5, 1, 10, 20, 10^2, 250, 10^3, and 10^6. The maximum CFL shown for the three-point method is the maximum value reported for all choices for the extra numerical boundary conditions investigated for the three-point scheme. As shown in Table III, the present method permitted significantly higher CFL values to be used for three of the five cases.

CONCLUSIONS

An implicit finite-difference method has been presented for obtaining steady-state solutions to the time-dependent quasi-one-dimensional Euler equations written in conservation form. The method uses a two-point difference scheme at subsonic points. At supersonic points, dissipation is added by the retarded density concept and the difference equations involve three points. However, the overall method retains the nice feature of general two-point methods as regards boundary conditions; that is, for subsonic inflow and outflow, the number of physical boundary conditions equals the number of boundary conditions required to solve the system of difference equations. In the present method, the outflow pressure is specified for all nozzle flows computed; thus, the method is very general in this respect. It was shown that this over-specification of the boundary conditions at a supersonic

outflow boundary was restricted to a thin "boundary-layer" region at the exit.

In general, it is concluded that:

(1) For subsonic inflow and outflow, with or without shocks, the present two-point scheme is preferred to a three-point scheme since it requires no extra numerical boundary conditions and these flows can be computed at CFL numbers on the order of 10^3 larger than the three-point method.

(2) For supersonic inflow, the present method requires boundary conditions at the first two entrance mesh points.

(3) For three of the five test cases, the present two-point method permitted calculations with much larger CFL numbers than the three-point method.

REFERENCES

1. Jameson, A.: Acceleration of Transonic Potential Flow Calculations on Arbitrary Meshes by the Multiple Grid Method. AIAA Paper 79-1458. Proceedings of AIAA 4th Computational Fluid Dynamics Conference, July 1979, pp. 122-146.

2. Moretti, Gino: Comment on "Stability Aspects of Diverging Subsonic Flows". AIAA J., vol. 19, no. 5, May 1981, p. 669.

3. Cline, M. C.: Stability Aspects of Diverging Subsonic Flow. AIAA J., vol. 18, no. 5, May 1980, pp. 534-539.

4. Yee, H. C.; Beam, R. M.; and Warming, R. F.: Stable Boundary Approximations for a Class of Implicit Schemes for the One-Dimensional Inviscid Equations of Gas Dynamics. AIAA Paper 81-1009. Proceedings of AIAA 5th Computational Fluid Dynamics Conference, June 1981, pp. 125-135.

5. Keller, Herbert B.: A New Difference Scheme for Parabolic Problems. Numerical Solution of Partial Differential Equations, II, Bert Hubbard, ed., Academic Press, Inc., 1971, pp. 327-250.

6. Keller, Herbert B.; and Cebeci, Tuncer: Accurate Numerical Methods for Boundary Layer Flows I. Two-Dimensional Laminar Flows. Proceedings of the Second International Conference on Numerical Methods in Fluid Dynamics. Volume 8 of Lecture Notes in Physics, Maurice Holt, ed., Springer-Verlag, 1971, pp. 92-100.

7. Wornom, S. F.: A Critical Study of Higher-Order Numerical Methods for Solving the Boundary-Layer Equations. AIAA Paper 77-637. Proceedings of AIAA 3rd Computational Fluid Dynamics Conference, June 1977, pp. 61-71.

8. Hafez, M.; South, J.; and Murman, E.: Artificial Compressibility Methods for Numerical Solutions of Transonic Full Potential Equation. AIAA J., vol. 17, no. 8, Aug. 1979, pp. 838-844.

9. Holst, T. L.; and Ballhaus, W. F.: Fast, Conservative Schemes for the Full Potential Equation Applied to Transonic Flows. AIAA J., vol. 17, no. 2, Feb. 1979, pp. 145-152.

10. Griffin, M. D.; and Anderson, J. D.: On the Application of Boundary Conditions to Time Dependent Computations for Quasi One-Dimensional Fluid Flows. Computers and Fluids, vol. 5, 1977, pp. 127-137.

11. Shubin, G. R.; Stephens, A. B.; and Glaz, H. M.: Steady Shock Tracking and Newton's Method Applied to One-Dimensional Duct Flow. J. Comp. Phys., vol. 39, 1981, pp. 364-374.

TABLE I.- PHYSICAL AND NUMERICAL BOUNDARY CONDITIONS FOR VARIOUS FLOWS

Class	Description	Boundary Conditions			
		Physical		Req'd. by Method	
		Inflow	Outflow	Inflow	Outflow
1	Subsonic inflow, subsonic outflow	1	1	1	1
2	Subsonic inflow, supersonic outflow	1	0	1	1
3	Supersonic inflow, subsonic outflow	2	1	2	1
4	Supersonic inflow, supersonic outflow	2	0	2	1

TABLE II.- SUMMARY OF FLOW CONDITIONS

Case	Nozzle Type	Description	Area Ratio
I	Convergent-divergent	Subsonic inflow, subsonic outflow (no shock)	2:1.16[a]
II	Convergent-divergent	Subsonic inflow, subsonic outflow (with shock)	2.5:1.5
III	Convergent-divergent	Subsonic inflow, supersonic outflow	2:2
IV	Divergent	Supersonic inflow, supersonic outflow	
V	Divergent	Supersonic inflow, subsonic outflow	

[a]Area ratio = 2:2 for the symmetric case

TABLE III.- EXPERIMENTAL MAXIMUM STABLE CFL NUMBER

Case	Present Method	Three-Point Method (Ref. 4)
I	10^6	10^3
II	10^6	20
III	10^6	10^6
IV	10^6	10^6
V	250[a]	10

[a]Unlimited CFL number can be used with "gradual start." (See text regarding Case V.)

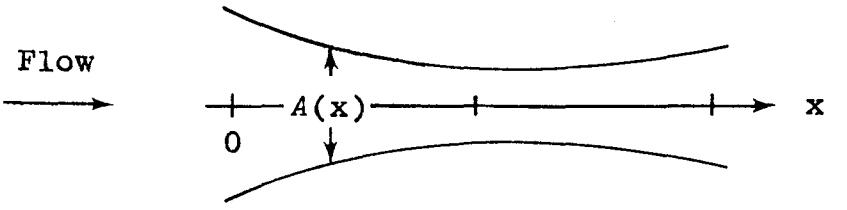

Figure 1.- Nozzle geometry.

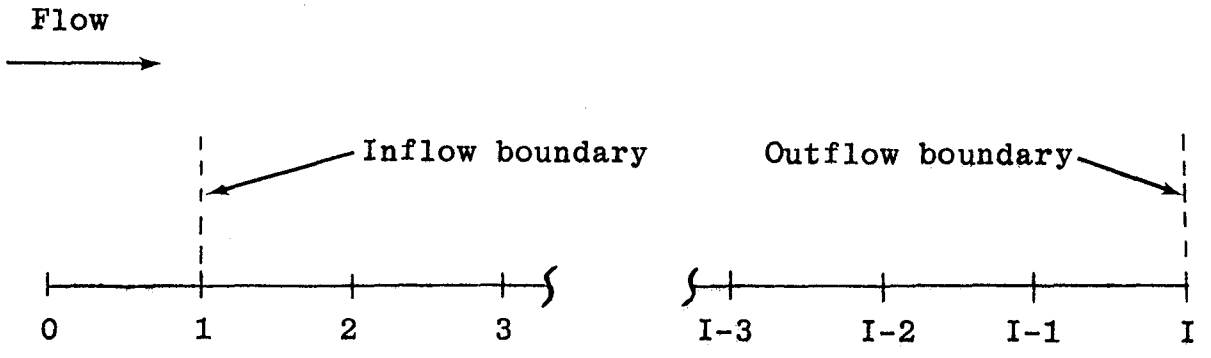

Figure 2.- Computational mesh.

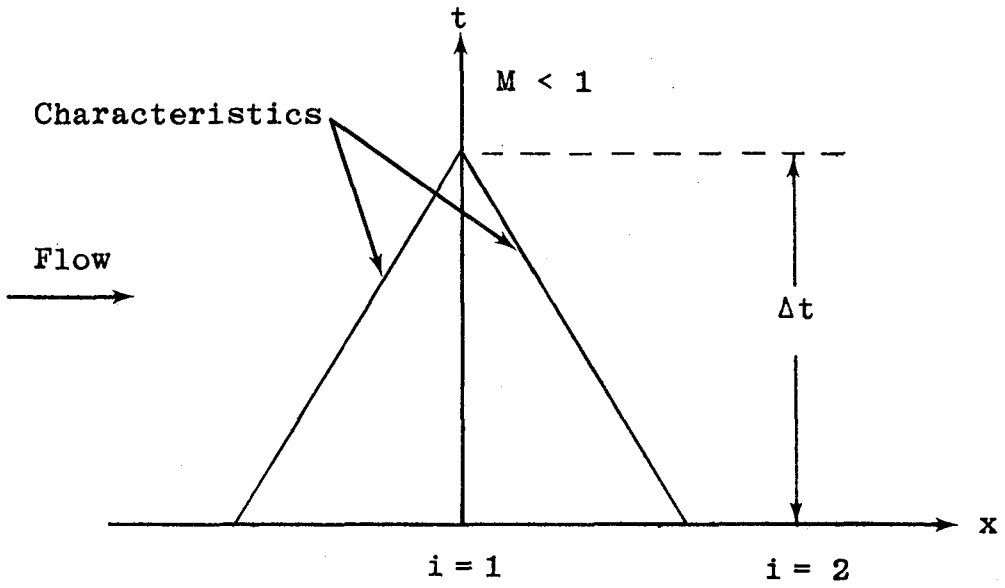

Figure 3.- Characteristics for subsonic flow.

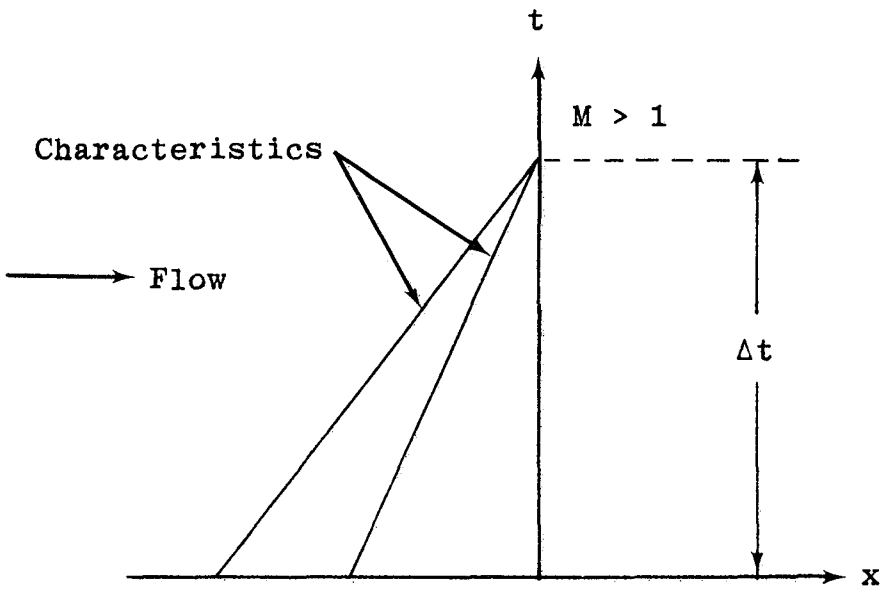

Figure 4.- Characteristics for supersonic flow.

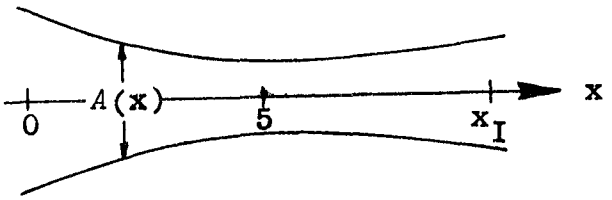

$$A(x) = A_{TH} + (A_0 - A_{TH})\left[(5 - x)/5\right]^2 \qquad x \leq 5$$

$$A(x) = A_{TH} + (A_I - A_{TH})\left[(x - 5)/(x_I - 5)\right]^2 \qquad x > 5$$

(a) Convergent-divergent nozzle (ref. 10) (A_0 = entrance area, A_I = exit area, A_{TH} = throat area).

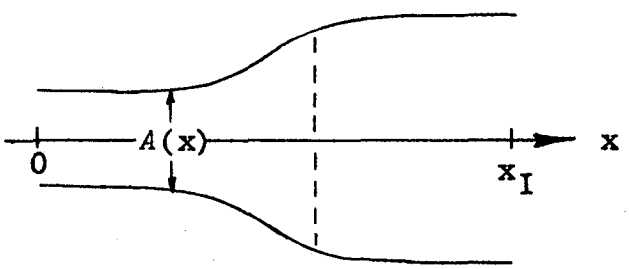

$$A(x) = 1.398 + 0.347 \tanh (0.8x - 4)$$

(b) Divergent nozzle (ref. 11).

Figure 5.- Nozzle geometry.

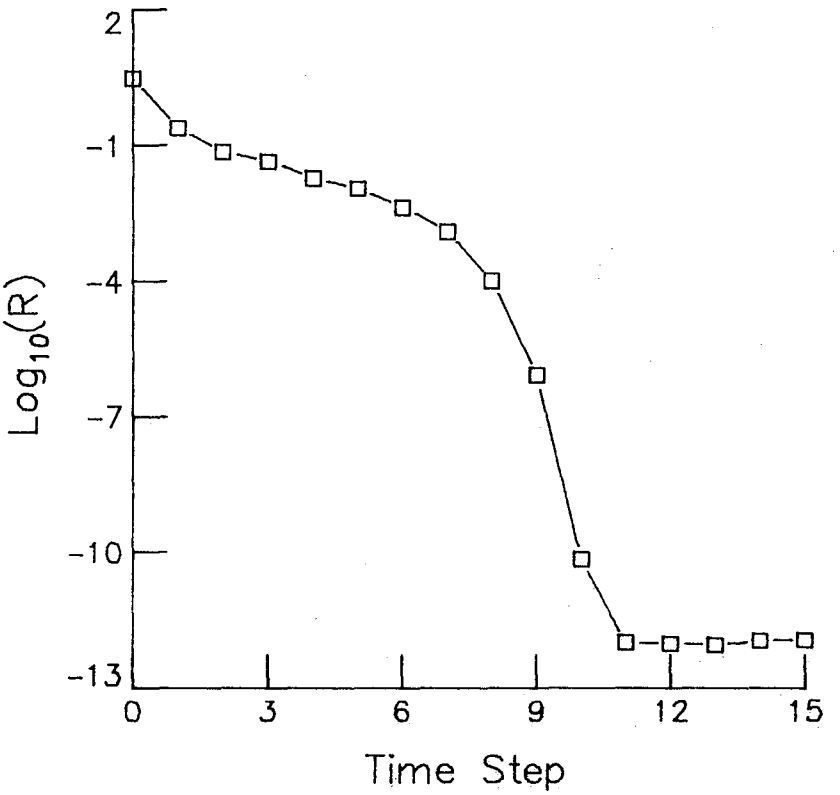

(a) Convergence history.

Figure 6.- Case I: Subsonic inflow, subsonic outflow, no shock ($CFL_{max} = 10^8$, 65-point grid).

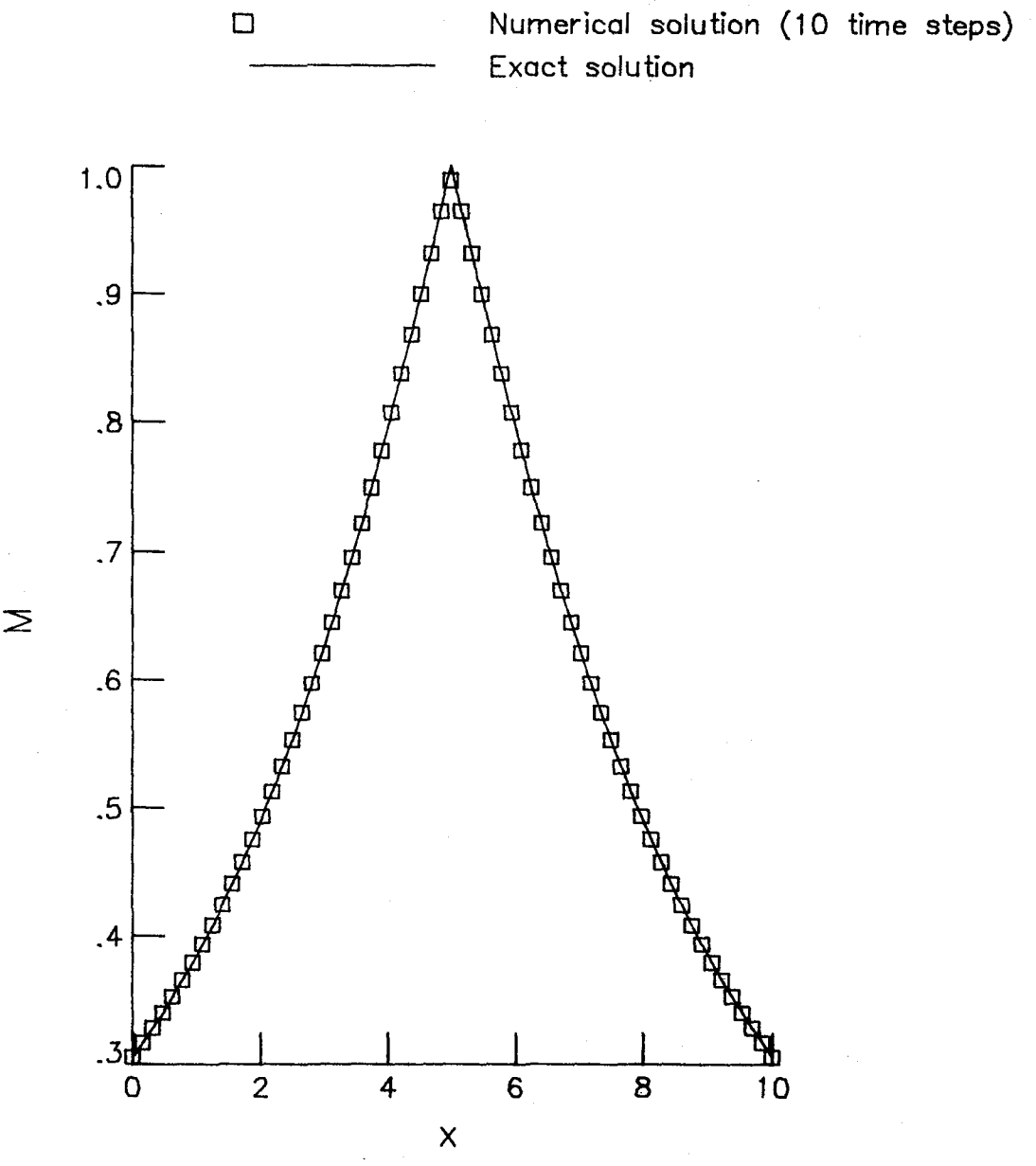

(b) Mach number.

Figure 6.- Concluded.

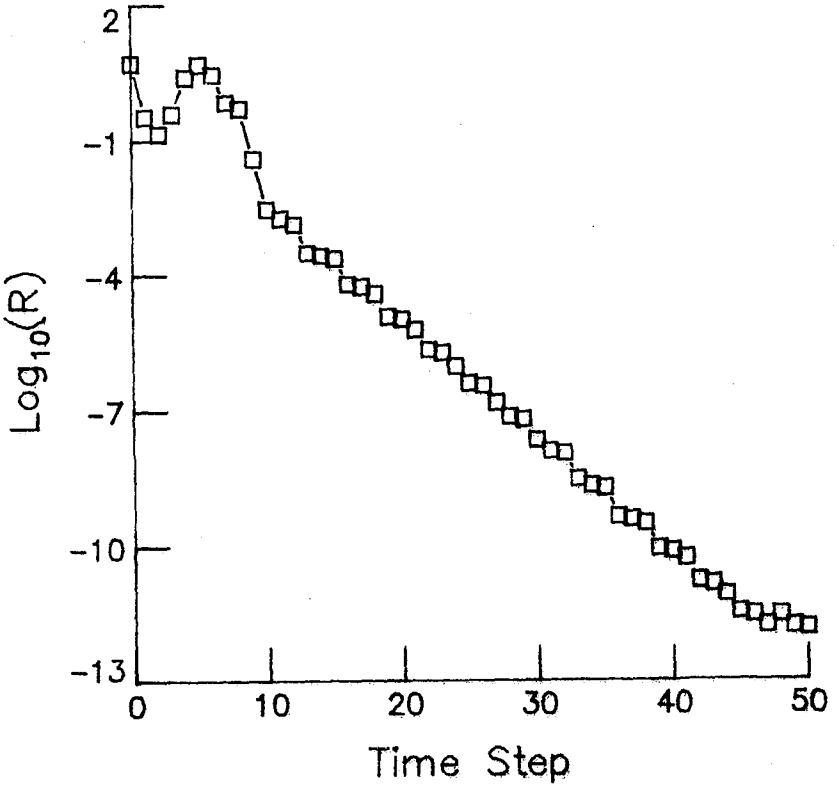

(a) Convergence history.

Figure 7.- Case II: Subsonic inflow, subsonic outflow, with shock ($CFL_{max} = 10^8$, 65-point grid).

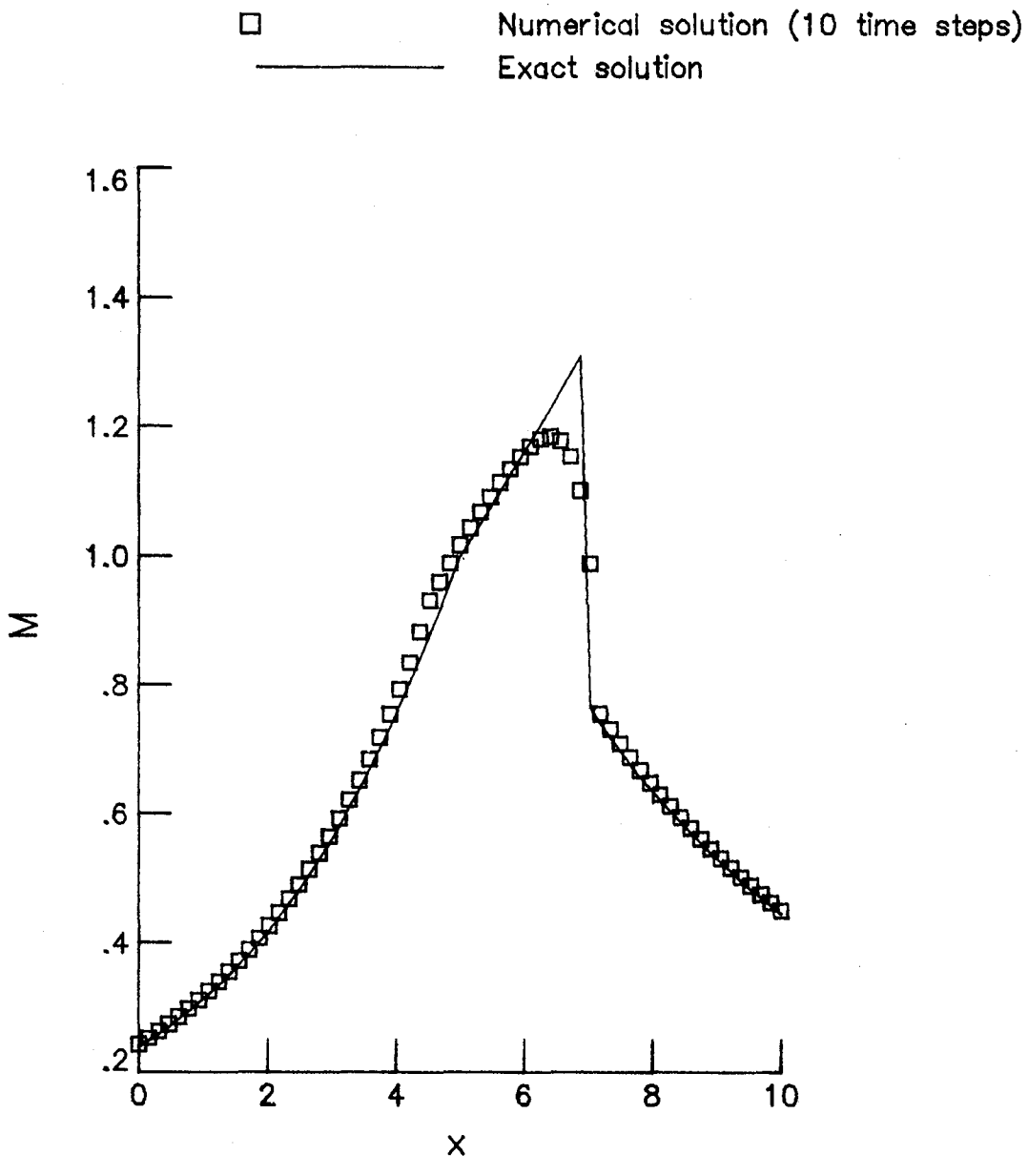

(b) Mach number.

Figure 7.- Continued.

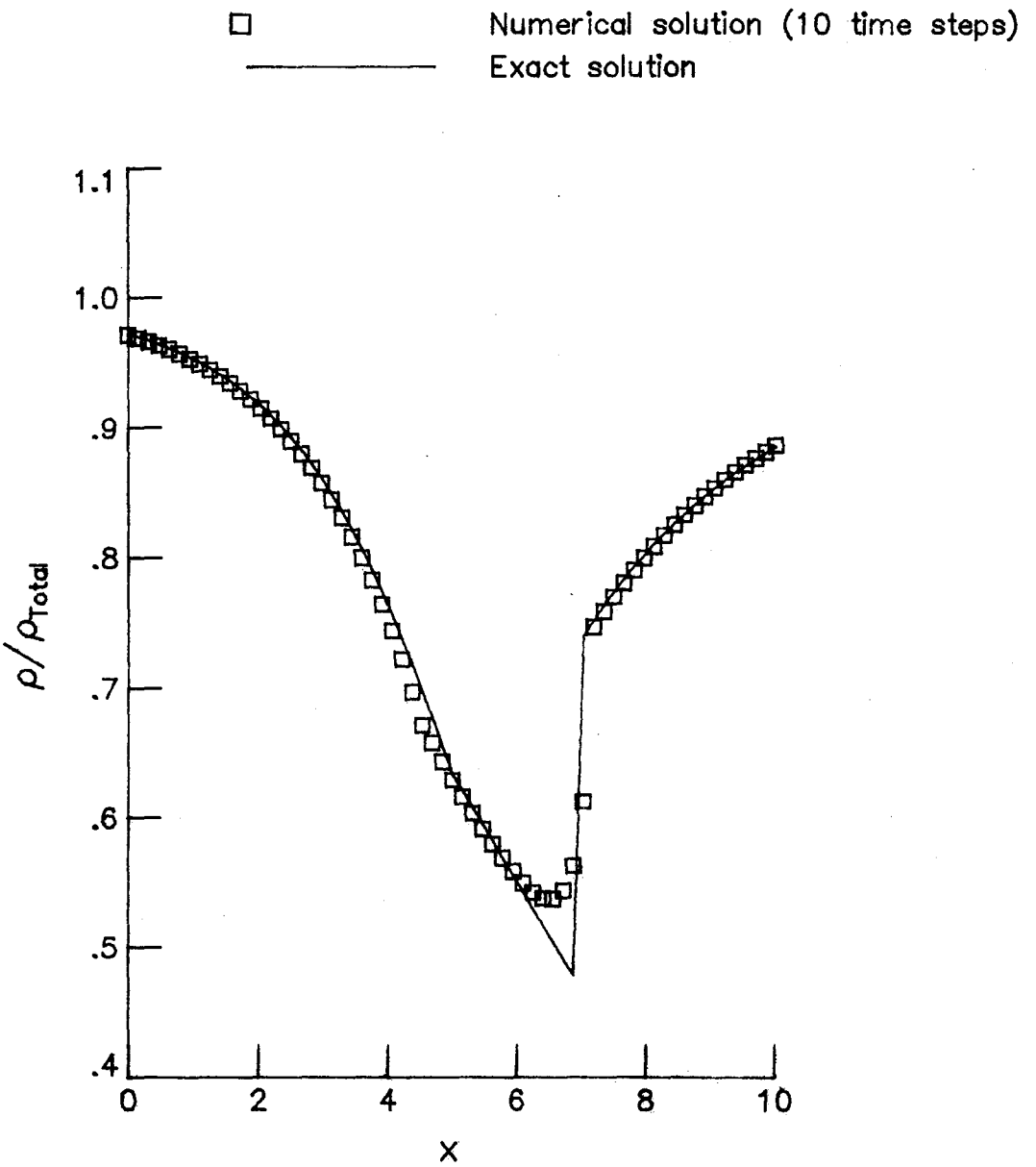

(c) Density.

Figure 7.- Concluded.

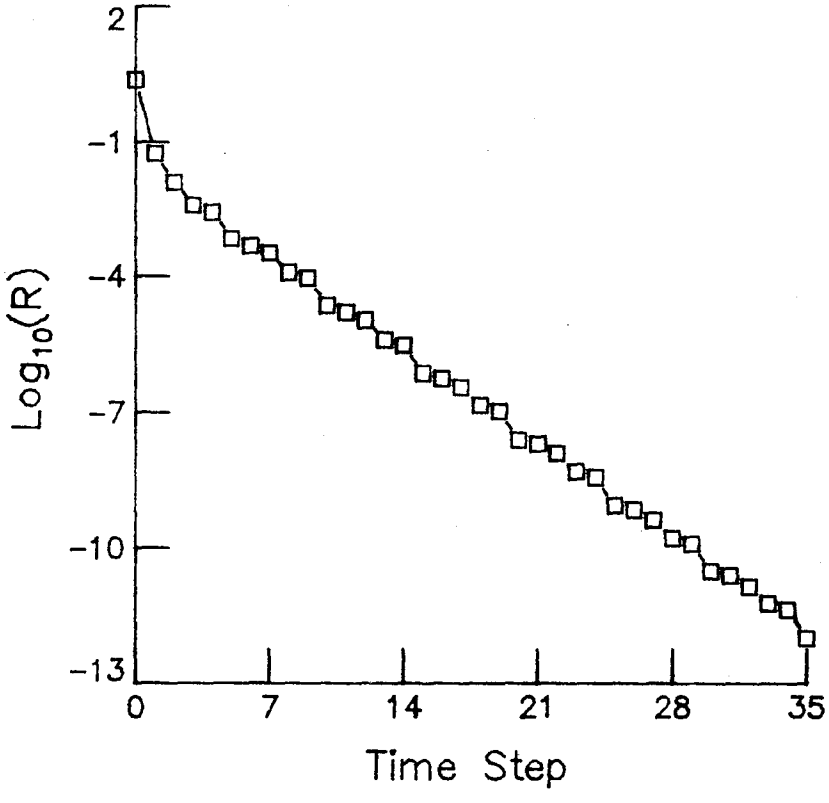

(a) Convergence history.

Figure 8.- Case III: Subsonic inflow, supersonic outflow ($CFL_{max} = 10^8$, 65-point grid).

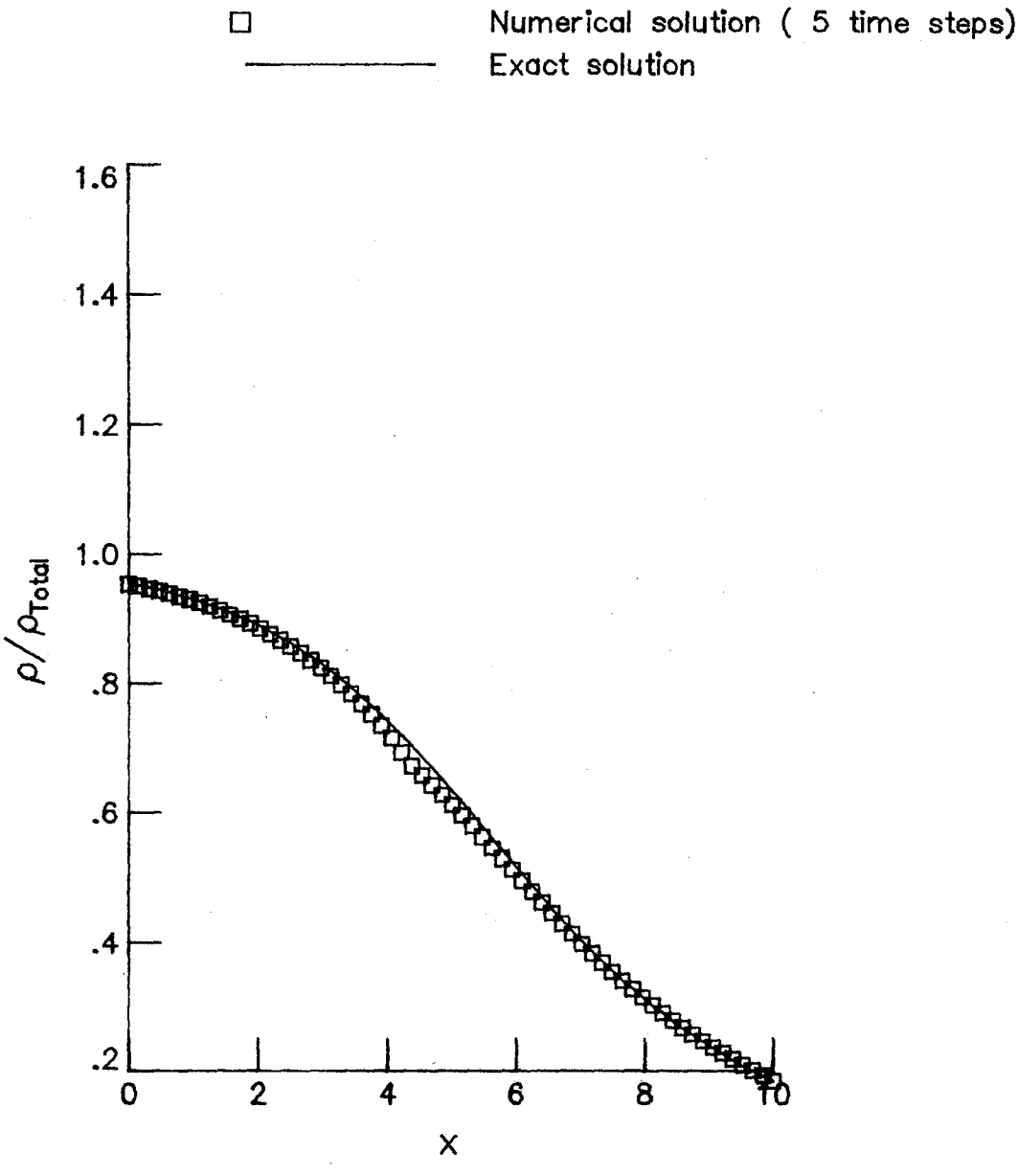

(b) Density.

Figure 8.- Concluded.

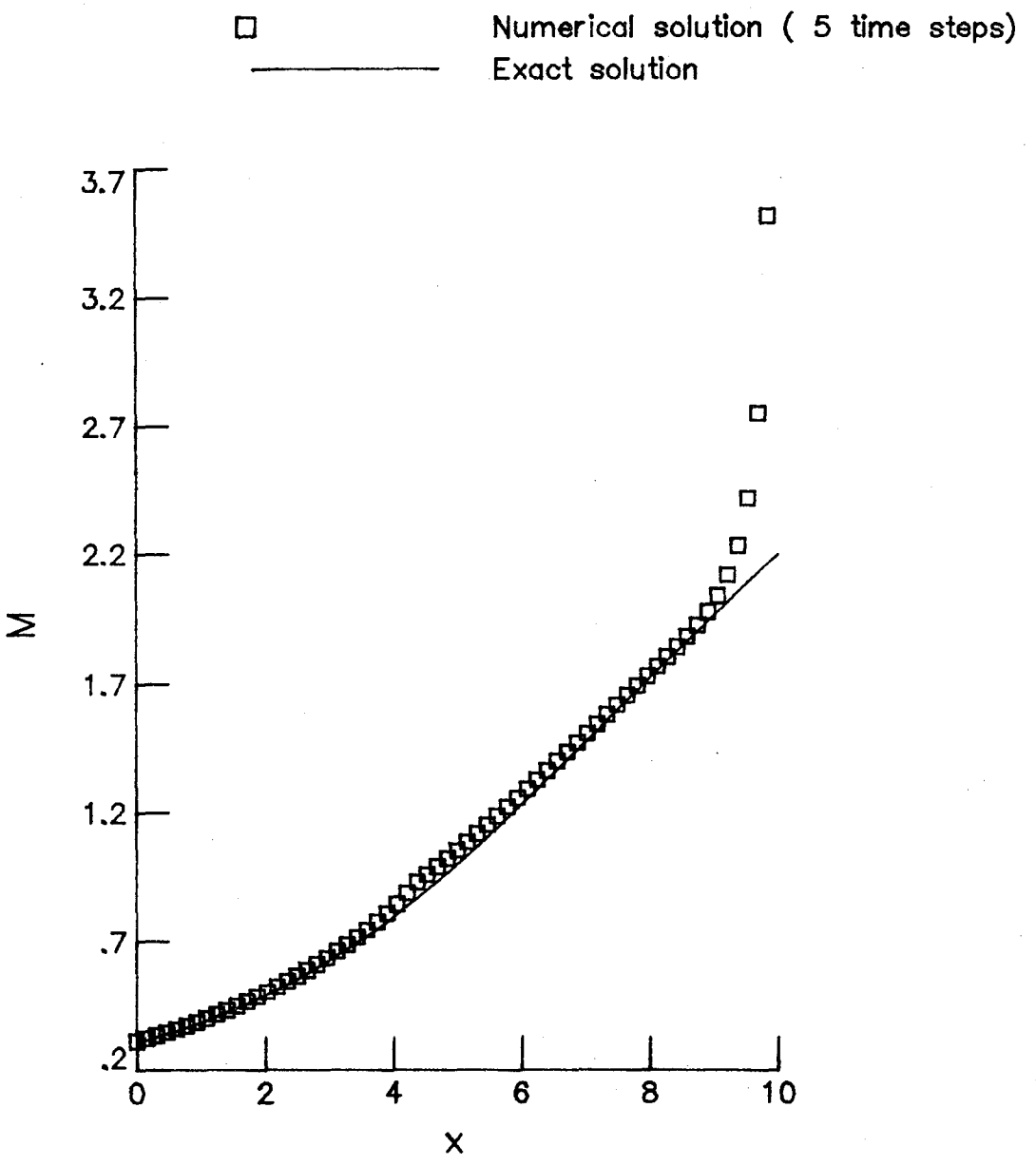

(a) Mach number.

Figure 9.- Case III: Subsonic inflow, supersonic outflow ($CFL_{max} = 10^8$, 65-point grid).

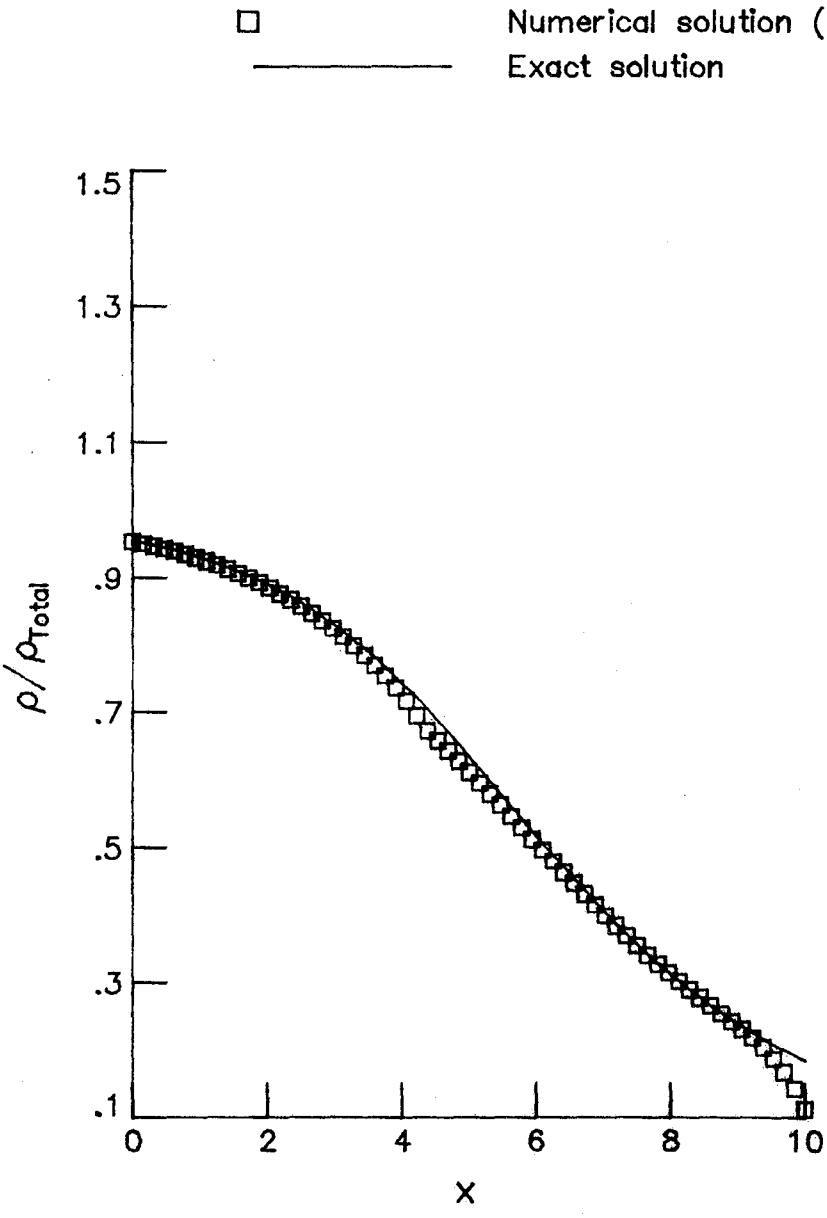

(b) Density.

Figure 9.- Concluded.

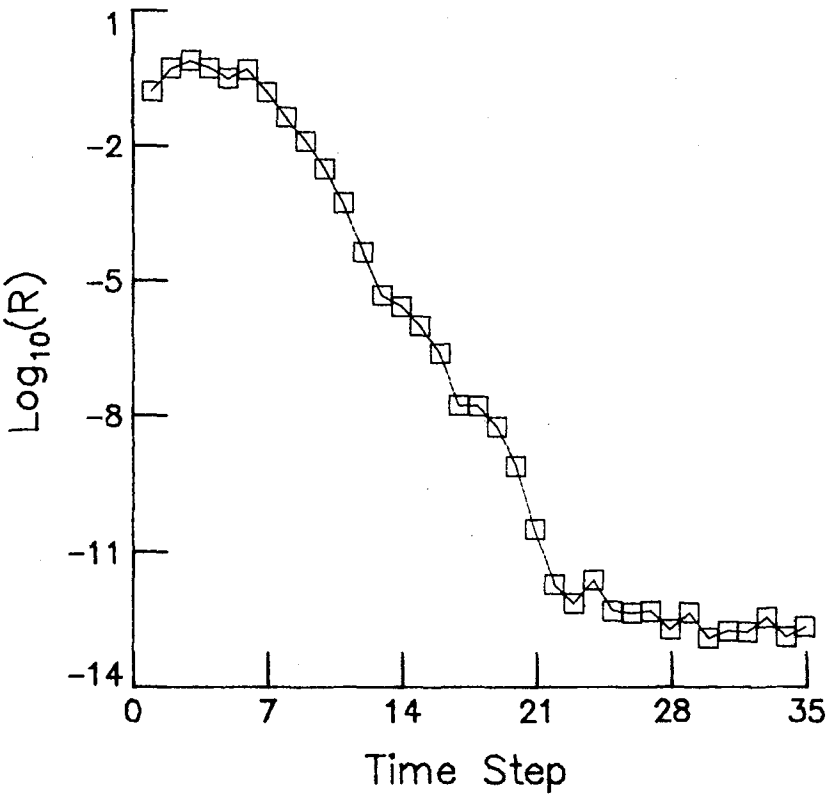

(a) Convergence history.

Figure 10.- Case V: Supersonic inflow, subsonic outflow (CFL_{max} = 250, 65-point grid).

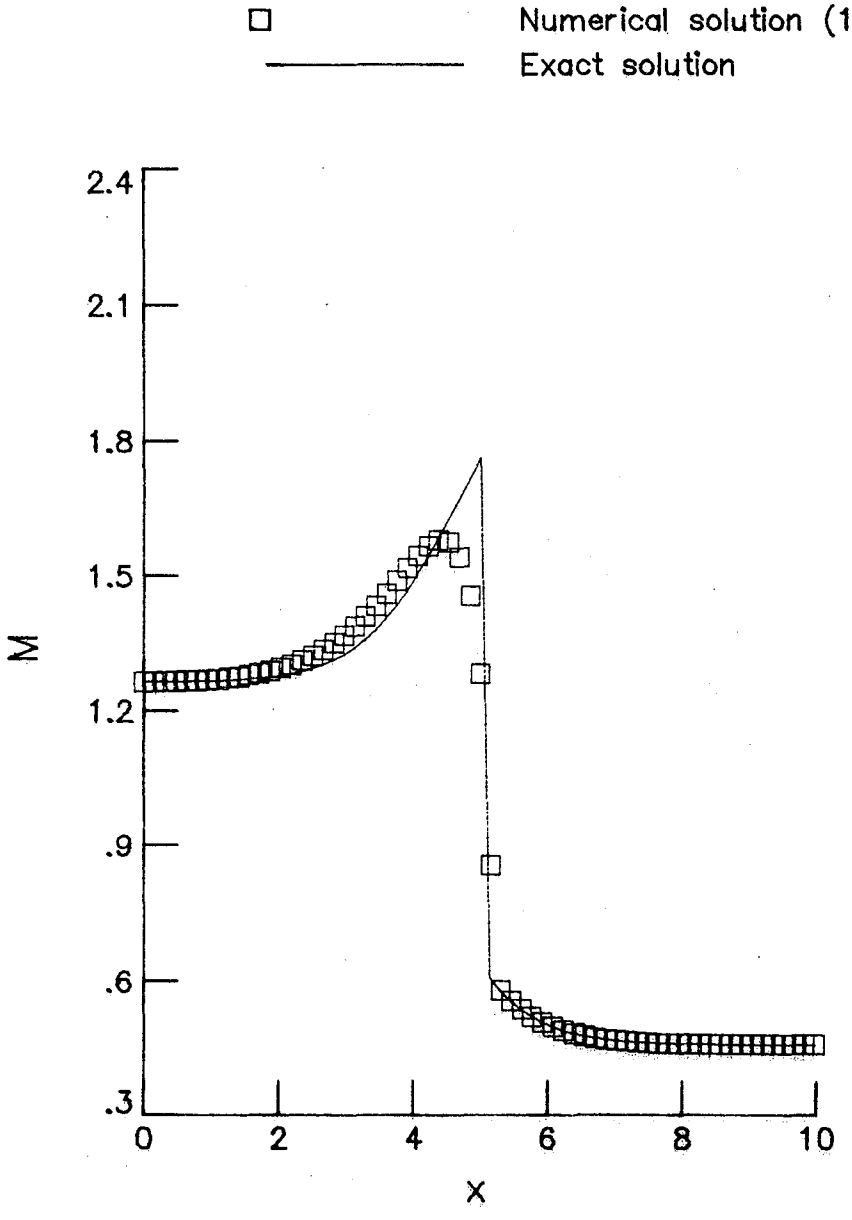

(b) Mach number.

Figure 10.- Continued.

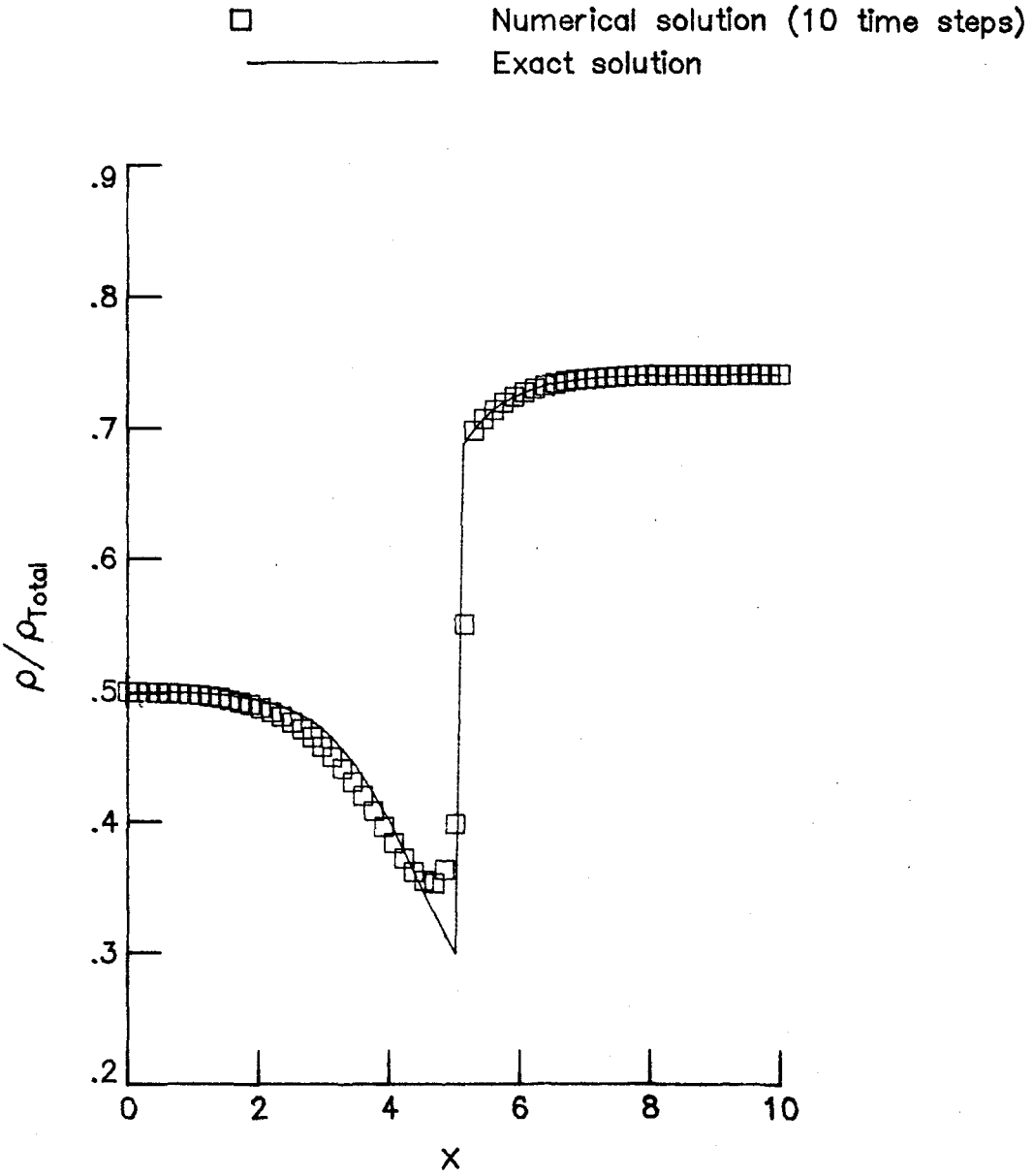

(c) Density.

Figure 10.- Concluded.

1. Report No.	2. Government Accession No.	3. Recipient's Catalog No.
NASA TM 83262		

4. Title and Subtitle	5. Report Date
APPLICATION OF COMPACT DIFFERENCE SCHEMES TO THE CONSERVATIVE EULER EQUATIONS FOR ONE-DIMENSIONAL FLOWS	May 1982
	6. Performing Organization Code 505-31-13-01
7. Author(s) Stephen F. Wornom	8. Performing Organization Report No.
	10. Work Unit No.
9. Performing Organization Name and Address NASA Langley Research Center Hampton, VA 23665	11. Contract or Grant No.
	13. Type of Report and Period Covered Technical Memorandum
12. Sponsoring Agency Name and Address National Aeronautics and Space Administration Washington, DC 20546	14. Sponsoring Agency Code

15. Supplementary Notes

16. Abstract

An implicit finite-difference method is presented for obtaining steady-state solutions to the time-dependent, conservative Euler equations for flows containing shocks. The method used the two-point differencing approach of Keller with dissipation added at supersonic points via the retarded density concept. Application of the method to the one-dimensional nozzle flow equations for various combinations of subsonic and supersonic boundary conditions shows the method to be very efficient. Residuals are typically reduced to machine zero in approximately 35 time steps for 50 mesh points. It is shown that the scheme offers certain advantages over the more widely-used three-point schemes, especially in regard to application of boundary conditions.

17. Key Words (Suggested by Author(s))

Euler Equations
Nozzle Flows

18. Distribution Statement

Unclassified - Unlimited

Subject Category 64

19. Security Classif. (of this report)	20. Security Classif. (of this page)	21. No. of Pages	22. Price*
Unclassified	Unclassified	44	

* For sale by the National Technical Information Service, Springfield, Virginia 22161